WOODS HOLE OCEANOGRAPHIC INSTITUTION

Woods Hole, Massachusetts

Reference No. 54-18

MARINE METEOROLOGY

Concerning the Structure of Some Cumulus Clouds which Penetrated the High Tropical Troposphere

By

Joanne Starr Malkus
and
Claude Ronne

Technical Report No. 27
Submitted to the Office of Naval Research
Under Contract N6onr-27702 (NR-082-021)

March 1954

APPROVED FOR DISTRIBUTION _____ Director

Abstract

Some extremely large oceanic trade-wind cumulonimbus clouds extending upwards of 40,000 ft. into a region of strong winds and intense vertical shear have been studied by means of time-lapse photography. A simultaneous still picture of the clouds taken a known distance and direction away from the motion pictures permits triangulation upon the clouds and calculation of the vertical and horizontal motions of several of the individual towers. By means of a nearby radiosonde observation, it is established that the air forming the strongest of these towers must have risen from near cloud base with little or no dilution of its buoyancy by mixing with the clear-air surroundings.

The model of Malkus and Scorer (1954) concerning the erosion of cumulus towers is reviewed and tested upon these towers with satisfactory results. A minimum horizontal cloud dimension is apparently required for the production of undiluted towers. The horizontal motion of the clouds relative to the air is also estimated from the model and tested by the observations and the net upward transport of latent heat in water vapor is calculated approximately.

I. INTRODUCTION

During the spring of 1953, a joint observational program was undertaken by the meteorological group from the Woods Hole Oceanographic Institution and the Department of Meteorology of the Imperial College, London. The over-all purpose of the program was the investigation of the structure of the low-level trade current and the transports therein of heat, water, and momentum, with considerable emphasis upon continuing the study of trade-wind clouds. Two main observation points were used, the first being the small, flat West Indian island of Anegada ($18^{\circ}50'$N, $64^{\circ}20'$W; dimensions two by ten miles) and the second a PBY-6A aircraft, equipped as a meteorological tool, which was flown in the near vicinity. The present paper reports some results of the cloud observation program.

The cloud program was divided into two main parts: the first consisted in airplane traverses through a single cloud following the methods developed by the Woods Hole group in the San Juan expedition of 1952 (reported upon in part by Malkus, 1954); and the second centered upon time-lapse motion pictures made from the island of Anegada. Two main objectives of the photography were to trace individual clouds through a large portion of their life history and to provide information on the interaction of groups of clouds, neither of which could be achieved directly by airplane measurements alone.

During the observation period from Anegada a particularly interesting synoptic situation was encountered on April 1, 1953. On this occasion several large cumulonimbus clouds reaching up to well over 40,000 ft. were observed far out over the ocean. Fortunately, not only were these clouds recorded by the time-lapse camera, but sufficient supplementary information was

available to permit numerous calculations from the films. After a brief description of the equipment and techniques used, the major portion of this paper will be concerned with these calculations and their interpretation.

The synoptic situation was dominated by the eastward passage on the preceding day of a strong polar trough. In the Caribbean area, the low-level easterlies were overlaid by westerlies beginning at 15,000 ft. elevation. These westerlies were concentrated in a shallow, high-tropospheric layer with maximum speeds of 100 mph at an elevation of 40,000 ft. The sequence of events is illustrated in the time section for San Juan, Puerto Rico (120 miles west-southwest from Anegada) shown in Figure 1. At the time of observation, 1220-1345 LST (1620-1745 GCT) the region was dominated by the northwesterly flow to the rear of the trough. By this time the overcast associated with the disturbance had broken sufficiently for several huge cumulonimbus clouds to be observed and photographed from Anegada. Fortunately the same clouds were simultaneously photographed with a still camera from the PBY, which was a known distance and direction from Anegada. Triangulation therefore permitted calculation of the distances, heights, and sizes of the clouds and their alteration with time from the motion picture film. The resulting horizontal and vertical motions could then be compared with the high-level wind and radiosonde observations which were taken a little over an hour earlier by the Weather Bureau at San Juan.

II. METHODS OF OBSERVATION AND CALCULATION

The time-lapse motion picture camera on Anegada was a Bolex 16 mm, equipped with an extreme wide-angle (58.3° horizontal, 44.3° vertical) lens. Exposures were made automatically at the rate of one frame every 3.6 seconds

or 1000 frames per hour. The camera was mounted on a tripod and aimed toward 22° from true North during the entire run.

The still camera in the PBY was a conventional Speed Graphic (50.0° horizontal, 42.0° vertical) which was mounted on gimbals so that it always remained level and was pointed at right angles to the fuselage. At the time the still pictures of the clouds were taken (1325 LST) the aircraft was flying at 6000 ft. elevation toward 293° True and was making a speed of approximately 130 mph over the ground. Since it was observed over Anegada on this heading at 1314 or 11 minutes earlier, a base leg for triangulation purposes of 24 miles is obtained. This distance was checked by additional knowledge of the time when the aircraft reached a location due north of San Juan. The base leg derived thus by interpolation came out 23 miles or within 5%. Correction of the base leg for wind drift of the aircraft was made, but was negligibly small.

Figure 2 shows the Speed Graphic (PBY) photograph used in the triangulation. The time-lapse pictures were printed at intervals of 1.2 minutes, and the prints numbered from the beginning to the end of the run (1-58). Selected prints from this series are reproduced in Figures 3 and 4. Print 44 was picked as the frame coincident with Figure 2. Triangulation was first performed for the three points marked with inverted arrows (on Figure 2 and Print 44) on the far cloud, hereafter to be called Cloud I. The angle of each point from the optical axis of the camera was found by using the proportional distance of the picked point from the center to the edge of the negative. The half-width of the negative and focal length of the lens were accurately known and these gave the tangent of the total half-angle covered by the camera.

Results of this and a similar triangulation on one point on the near cloud (called Cloud II) are shown in Figure 5. By laying out two angles for each point at the ends of the base leg on a scaled map, it was determined that the three points in Cloud I lay not only in a straight line but almost exactly parallel to the image plane of the motion picture camera (i.e. in the plane of the photographs) and a perpendicular distance from it of 78 miles. The point on Cloud II was a perpendicular distance of 66 miles from the image plane. After discussing the possible errors in triangulation, we may carry out calculations from this point forward using the motion picture frames alone.

In the case of Cloud I, for which all the significant calculations were performed, the image location never exceeded an angle of $\pm$ 10° from the optical axis, hence errors in distances and separations due to distortion by the lens may be totally neglected compared to errors in triangulation. An error of 2.2 miles in the base line (9%) would give an 8% error in the distance to Cloud I, and it is doubtful that the error in the base line was this great. The largest source of error lies in the determination of the angles. A 2° error in any one of the angles would produce a 7 mile or 9% error in distance to Cloud I. All the angles save one may be shown reliable within this accuracy. The greatest uncertainty lies in the angle between the optical axis of the Speed Graphic and the heading of the PBY, which was adjusted to 90° by sighting along the trailing edge of the wing (fortunately constructed at exactly 90° to the aircraft axis). That the errors in angle were very small, however, is suggested by several independent checks upon the triangulation. The first is that all three points on Cloud I lie in a straight

line along the plane 290°-110°, as an analysis using the wind profile shows must be the case. The second is that triangulation gives horizontal separations on the map between these points departing by much less than 10% from the separations measured on the photographs, using the derived distance to the camera of 78 miles. The final check is that triangulation on Cloud II gives its heights and velocities as extremely close to those of comparable portions of Cloud I.

The vertical angular distance (on Print 44) between the horizon and the farthest left point on Cloud I is determinable from the ratio of this distance to the vertical half-width of the negative and knowledge of the focal length of the lens. Using the horizontal distance of 78 miles and the tangent of this angle, the vertical elevation of this point above the horizon was found to be 27,000 ft. or 8.24 km. This length could then be used as a basic distance scale for the calculations to follow. In order to obtain the elevation of this point above sea level, however, a correction had to be introduced due to the curvature of the earth. For a distance of 78 miles, this proved to be 4000 ft. or 1.2 km. In presenting actual altitudes of all points on Cloud I, this correction has been added.

In order to apply the distance scale obtained from Print 44 to other parts of the cloud and to motions of portions of the cloud towers throughout the entire 70-minute run, it was first necessary to ascertain whether the cloud had any component of motion into or out of the plane of the photograph and whether it might develop any slope normal to that plane. Inspection of the San Juan radio-wind observation (see Figures 1 and 6) shows that the wind directions throughout the height range of the calculations (30,000-47,000 ft.) departed rarely, and never more than by 10°, from the plane of

the photographs. Although the wind departed significantly from this direction at lower levels, it may be shown by consideration of even the minimum horizontal drag forces ordinarily acting on cumulus that the component of cloud motion normal to the photographs should have become vanishingly small by 9.5 km. Thus the distance scale for Print 44 was used throughout without correction, with extremely consistent results. The Appendix considers the applicability of the San Juan soundings to the time and location of the clouds, and shows that possible changes in wind and thermal structure were probably too small to disturb the calculations.

III. RESULTS OF SOME VELOCITY CALCULATIONS

Some of the basic dimensions of Cloud I are readily obtainable from Print 44. At 31,000 ft. (9.5 km), the width of the left-hand tower (containing the left-most point triangulated) is 20,500 ft. or 6.3 km. The greatest elevation above sea level attained by the cloud is reached by the streamer extending out to the right which has a maximum height of about 15.3 km or 46,600 ft. and a horizontal extent of 45 miles. The striking feature of this cloud's changes with time on Prints 1-58 (70 minutes) is its production of successive towers, each of which is seen to rise vertically, spread laterally into a long streamer and then dissipate gradually. On four of the more vigorous of these towers, vertical and horizontal speeds were calculated on the topmost point as it rose. The calculation for the tower marked X on Prints 37, 40, and 44 (Figures 3d, 4a, and 4b, respectively) is probably the most accurate, due first to coincidence with time of triangulation and second to the ease with which a readily identifiable portion of the tower could be traced from one frame to the next. The result of the calculation is presented in Table I.

Table I

Heights and Velocities for Tower X, Cloud I

Print number	Time Interval minutes	Height ft	Height km	w mps	u_c mps	u_E mps	$u = u_E - u_c$ mps
33		31,000	9.45				
	2.4			10.5	17.0	32	15.0
35		35,900	10.95				
	2.4			7.1	28.5	38.5	10.0
37		39,200	11.96				
	2.4			2.7	19.5		
39		40,500	12.35				
	3.6			1.1	27.5		
42		41,200	12.58				
	4.8			1.1	29.0		
46		42,400	12.90				

The vertical rate of ascent, w, of the tower top was obtained merely by subtracting the two heights and dividing by the time interval, and is thus an average between the frames indicated. The horizontal velocity, u_c, of the tower top was obtained similarly by subtraction of two successive horizontal positions. The external wind, u_E, was read from Figure 6 at a level midway between the two elevations, at which heights X's were plotted showing the calculated value of u_c. The drop in u_c between 11.96 and 12.35 km may be inferred to be due to evaporation of the cloud streamer from its forward end. From the film and the computed velocities for 9.50-11.96 km, however, it appears that the tower is moving without evaporation and hence its speed may be inferred to be the same as that of the updraft for the lowest two X's on Figure 6. The relative horizontal velocities, $u = u_E - u_c$, are to be used later in examining the frictional interaction between cloud tower and surroundings.

Two additional cloud towers on Cloud I proved traceable throughout their life histories. The first of these appeared in Prints 6-27 and is marked by horizontal bars on Figures 3a, b, and c. This tower reached the greatest height, as will be brought out in the following section, and exhibited the largest cross section of all of them. The pertinent calculations are presented in Table II. Due to the considerable width of the tower, its horizontal motion could not be determined with great reliability after Print 9.

Table II

Heights and Velocities for Tower Y, Cloud I

Print	Time Interval	Height	Height	w	u_c
number	minutes	ft	km	mps	mps
6		34,800	10.60		
	3.6			8.4	25.2
9		40,700	12.40		
	3.6			1.9	28.2
12		42,000	12.80		
	3.6			1.4	35
15		43,100	13.10		
	3.6			1.2	32
18		43,900	13.35		
	10.8			0.3	indeterminate
27		44,400	13.55		

These values of u_c are shown as horizontal bars on Figure 6 at the mean of the two indicated elevations.

The third tower was considerably weaker than the two previous ones, and dissipated at a considerably lower elevation. It appeared on Prints 21-35 and is shown by the inverted triangle on Figure 3c. The pertinent calculations are presented in Table III.

Table III

Heights and Velocities for Tower Q, Cloud I

Print	Time Interval	Height	Height	w	u_c	u_E	$u = u_E - u_c$
number	minutes	ft	km	mps	mps	mps	mps
21		31,200	9.5				
	2.4			7.0	13.5	22.5	9.0
23		34,500	10.5				
	2.4			3.5	24.0	37.0	13.0
25		36,100	11.0				
	2.4			2.1	24.0	39.0	15.0
27		37,200	11.32				
	2.4			1.1	26.0		
29		37,650	11.49				
	7.2			0.8	20.0		
35		38,850	11.84				

The values of u_c are plotted at the appropriate heights on Figure 6 using inverted triangles.

In addition an early tower, called W, on Cloud I was studied, but it was closing its life cycle at the beginning of the run and hence it is not presented here in detail. Its horizontal velocities, however, are entered as squares in Figure 6, and it is shown by the streamer with a square above on Figures 3a and b. The streamer on Cloud II was also followed (shown by triangles on Figures 3c, d, and 4a, b, c, and d) and its horizontal velocities are given by the triangles at the appropriate heights on Figure 6. This calculation was continued up to higher elevations than were the towers on Cloud I merely because the cloud fragment was easier to detect. Some of the streamers from Cloud I attained equally great elevations.

Now a physical interpretation of some of the foregoing observations may

be possible. It is important to note that the three towers described here underwent an initial period of rapid rise which petered out into a period of much slower rise somewhere between about 11.0 and 12.5 km. In the case of the most vigorous towers, X and Y, close inspection of the films reveals that this transition took place very near to 12.2 and 12.6 km, respectively, where the appearance of the towers also changed markedly and sharp outlines became lost. This transition could be in no way related to the transition between super-cooled water and ice crystals which must have occurred at no higher than 10.9 km, where even the most buoyant possible cloud element reached -40.0°C.

The San Juan radiosonde observation for 1500 GCT is reproduced in Figure 7. The sounding has a most striking feature. It shows that any cloud element which is finally to reach the vicinity of 12.5 km with vanishing (and not negative) buoyancy must have risen moist adiabatically and undiluted all the way from cloud base at 950 mb. Any mixing or dilution by the clear-air surroundings on the way up, even a small fraction of that encountered by Stommel (1947), Malkus (1952, 1954) and others in smaller trade cumulus would result in prohibitively large negative buoyancies at this level. The next section is intended to shed light upon this point.

IV. THE EROSION AND LIFE CYCLE OF THE CLOUD TOWERS

a) The Model To Be Used

The successive production by a cumulus of isolated towers, and their subsequent dissipation, is a situation clearly inappropriate for the application of a steady-state cloud model. A theoretical framework for describing the erosion of such transient towers has, however, recently been worked

out by Malkus and Scorer (1954) in a paper hereinafter referred to as I. The present observations provide material for the further testing and possible extension of their model. These authors treated cumulus towers as isolated, buoyant air bubbles which eroded as they rose, each closing its individual life cycle when totally eaten away.

The study of large buoyant bubbles in application to geophysical problems was commenced by G. I. Taylor (Davies and Taylor, 1950; Taylor, 1950). Davies and Taylor studied air bubbles rising through water and showed that the observed limiting velocity of rise could be obtained by assuming potential flow around the spherical upper surface of the bubble. This limiting velocity is reached because the buoyancy of the bubble is balanced by the drag exerted by the surrounding fluid as it is deflected around the cap. Taylor (1950) applied his results to buoyant air bubbles in air in the case of the atomic bomb cloud with surprisingly high accuracy. Scorer and Ludlam (1953) suggested that the bubble model could be applied with value to ordinary convective elements, such as thermals and cumulus clouds, and presented evidence that cumulus towers showed both the required rounded tops and approximated a limiting velocity. They added the idea of erosion, hypothesizing that air bubbles in air would retain the near-spherical cap by a continuous shedding of their outer skin, which sank relatively and became incorporated into the wake. That spherical-capped, bubble-like buoyant elements may arise spontaneously in a convecting fluid has been noted by W. Malkus[1] in his extensive laboratory experiments (1954) on a fluid heated from below.

In paper I, a quantitative law for the erosion of atmospheric bubbles

---

[1] Conversations with the writers.

was put forward and tested. This law states that

$$\frac{dR^3}{dt} = -3ER^2gB \tag{1}$$

where R is the radius of curvature of the bubble, E is a constant of proportionality called the erosion constant, and gB is the buoyancy acceleration, where $B = \Delta\rho/\rho$, $\Delta\rho$ being the bubble's density deficiency with respect to that of the environment of density ρ.

If the buoyancy of the bubble is constant, that is, when the environment has a wet adiabatic lapse rate, we may readily integrate (1). Using the boundary condition R = 0 at t = 0, and considering negative time decreasing during the bubble's life, this integration gives

$$R = -EgBt \tag{2}$$

or a linear decrease of radius with time is hypothesized. This erosion law was combined with an equation of motion for unit mass of the bubble, namely

$$\frac{dw}{dt} + Kw^2 = gB \tag{3}$$

where

$$K = \frac{9}{4R} \tag{3a}$$

A differential equation of this form may be shown applicable to cloud towers provided only that they retain a quasi-spherical top and do not erode so fast that the actual velocity departs radically from the limiting velocity w_o.

The limiting velocity may be found from equation (3) by setting dw/dt, hereafter called $\dot{w}$, equal to zero, viz.

$$w_o = \frac{2}{3} (gBR)^{\frac{1}{2}} \tag{4}$$

which is the same expression derived and tested by Davies and Taylor (1950) when $B \approx 1$.

When the erosion law (2) is substituted into the differential equation (3) and the result solved for E we have

$$\frac{3}{2} E^{-\frac{1}{2}} \equiv G = \frac{(-t)^{\frac{1}{2}} gB \, (1 - \dot{w}/gB)^{\frac{1}{2}}}{w} \tag{5}$$

If the hypothesized laws are valid, $3/2E^{-\frac{1}{2}}$ or G should be constant for all cloud towers which are sufficiently isolated to be treated as individual bubbles. Equation (5) is ideally suited to test by calculations from time-lapse motion pictures, if the buoyancy gB is known or can be estimated and does not vary too rapidly with time. It was shown in I (see Section IIb and Appendix I, loc. cit.) that equation (5) could be used with varying values of buoyancy provided that the buoyancy did not vary by more than 1/3 in 100 seconds. An increase in buoyancy at this rate might overestimate G by as much as 20%. It should be pointed out that from the level of their formation upward, the cloud bubbles are hypothesized to be rising along a wet adiabatic, mixing with the environment being achieved by erosion and wake production, the core remaining undiluted until its final disappearance. The bubbles studied in I were found to originate at different levels, some over

land forming at or near the ground, others at cloud base, and still others up to the highest level within the cloud where the external lapse-rate exceeded moist adiabatic. No trade cumulus bubbles were found in that study which originated below cloud base. The ones formed at higher levels were generally composed of smaller ones plus wake material, and thus were more "dilute" or had less buoyancy than those forming lower down.

Tests performed in I upon small and medium-sized cumulus bubbles showed that G was constant to an excellent degree of accuracy, both during the life of a single cloud tower and from tower to tower, regardless of location or external conditions. The mean value of G came out 0.2, giving an E of about 50 seconds. The highest-penetrating bubble studied was a trade cumulus tower reaching 16,000 ft. which did not, however, become glaciated.

b) The Life Cycles of Individual Towers

The cloud towers in the present study not only reached great heights, but penetrated tremendously high wind shears and definitely contained ice crystals throughout a significant portion of their life histories. It should be of considerable importance to determine whether equation (5) and the constant value of E obtained for the bubbles studied in paper I give here also a consistent relation between velocity, acceleration, buoyancy, and time. If so, it will be of interest to see how the present observations may be interpreted and clarified by means of this model. Most of the present towers have the advantage of being well isolated from interference by one another due to great wind shear and thus form an especially valuable test case.

To make this test, the original motion picture film was projected on a

microfilm viewer, from which the heights of the bubble tops were read off at every frame (3.6 sec). Although the vertical resolution was still smaller than desirable, there being commonly only about 1 cm height difference between the emergence of a bubble and its death as an entity, the results of drawing a smooth curve through the points were extremely satisfactory. The measurements and method of calculation of velocities and accelerations for Tower X are shown in Figure 8. A dual criterion was used for picking the time of complete erosion, when (-t) was to be set equal to zero, as described earlier in I. This time was chosen when the levelling off of the ascent was indicated on the graph, coincident with a fuzzy appearance and loss of clear-cut edges showing itself on the film. In applying and testing equation (5) on Tower X, therefore, the quantities w, $\dot{w}$ and -t were taken from the curves shown in Figure 8. It was then desired to see whether reasonable and observationally supportable values of gB, the bubble's buoyancy, could give rise to values of G which both remained nearly constant throughout the bubble's life and averaged about 0.2 $sec^{-\frac{1}{2}}$ as established for the bubbles in paper I. When the values of buoyancy are chosen with the aid of the sounding in Figure 7, under assumptions to be described presently, the resulting calculations of G are obtained which are shown in Table IV. Under these conditions the average G, or $\bar{G}$, is 0.195 $sec^{-\frac{1}{2}}$ and the percentage spread in G, called $\triangle$, is only 25%.

The values of buoyancy in the column marked gB in Table IV may be obtained for this bubble from the sounding in Figure 7 under several assumptions, the most crucial being that the San Juan radiosonde observation is applicable to the clear-air environment of the clouds. This point is

Table IV

Tower X, April 1, 1953

Height range studied 10.42-12.24 km

Observation number	$-t$ sec	$(-t)^{\frac{1}{2}}$ $sec^{\frac{1}{2}}$	w mps	$\dot{w}$ cm/sec^2	gB cm/sec^2	$\dot{w}/gB$	$(1-\dot{w}/gB)^{\frac{1}{2}}$	G $sec^{-\frac{1}{2}}$
1	288	17.0	11.7	-2.2	14.0	-.157	1.08	0.22
2	270	16.5	11.2	-2.2	13.3	-.165	1.08	0.21
3	252	15.9	10.5	-2.2	12.7	-.173	1.08	0.21
4*	234	15.3	9.8	-2.2	11.5	-.190	1.09	0.20
5	216	14.7	9.2	-2.2	10.4	-.210	1.10	0.18
6	198	14.1	8.3	-2.8	9.0	-.310	1.15	0.18
7	180	13.5	7.2	-2.8	8.8	-.320	1.15	0.19
8	162	12.8	6.4	-3.0	8.6	-.350	1.16	0.20
9	144	12.0	5.8	-3.0	8.4	-.360	1.17	0.20
10	126	11.2	5.5	-2.2	8.2	-.270	1.13	0.19
11	108	10.4	5.3	-2.2	8.0	-.280	1.13	0.18
12	90	9.5	4.7	-3.0	7.8	-.385	1.18	0.19
13	72	8.4	4.4	-3.0	7.6	-.395	1.18	0.17
14	54	7.4	3.9	-3.8	7.6	-.500	1.23	0.18
15	36	6.0	3.0	-4.8	7.6	-.630	1.28	0.19
16	18	4.2	2.0	-6.2	7.6	-.820	1.35	0.22

*Bubble diameter measured as 1.33 km

$\bar{G} = 0.195$
$\Delta = 25\%$

established in the Appendix. The second assumption is that the ascent curve of the bubble forming Tower X is very closely given by the dashed (right-hand) moist adiabat on Figure 7, which originates from the environment sounding at cloud base level. That this curve delineates the maximum possible buoyancy for this tower is supported by other work on oceanic trade cumuli (Malkus, 1954) showing that cloud buoyancies at cloud base level rarely exceed that contributed by water vapor alone. It will be noted that this adiabat re-crosses the sounding curve just above 12.5 km, leaving the bubble some buoyancy at its demise at 12.24 km. Thus this adiabat, according to the bubble model, also represents minimum buoyancy for this tower since isolated bubbles cannot continue to rise without positive buoyancy. In proceeding from the virtual temperature differences between the dashed adiabat and the sounding curve to the values of gB presented in Table IV a negative correction to the buoyancy due to the presence of suspended hydrometeors has been introduced. This correction allows for about 4.5 gm/m^3 of water or ice particles at 10.42 km, diminishing to 2 gm/m^3 at the bubble's demise at 12.24 km. This correction amounts to nearly 30% of the total buoyancy and is both uncertain and arbitrary: it is simply delimited by that reduction in buoyancy necessary to proceed from the dashed adiabat to the values of gB in the Table which produce values of G consistent with those in paper I. That these figures are not unreasonable, however, may be seen as follows: if all hydrometeors were being retained in the bubbles from cloud base upward, the water or ice content at 10.5 km would be about 18 gm/m^3. These clouds were, however, observed to be precipitating heavily from their bases. Thus a hydrometeor content from 10-25% this figure is plausible, especially when it falls within the range of observed water contents in large cumuli.

The latent heat of freezing has been ignored in the present computation, the assumption being that most of the freezing took place below 10.42 km where the bubbles began to be tracked.

Tower Y was treated in a similar manner as Tower X and the results are presented in Table V. The buoyancy used in this table was obtained also using the dashed adiabat in Figure 7, with the same magnitude correction for weight of hydrometeors. It should be pointed out that Tower Y was composed of several bubbles of the size of the one tabulated, which accounts for its great width. In Figure 3a, four of these are plainly visible. The bubble studied is the right-hand one which ascended first. However, it will be noted that the arrival of successors disturbed the constancy of G, especially from t = -210 sec on. This was due to overly large ascent speeds acquired by this bubble due to being pushed up by successors, resulting in a too low value of G. The same effect was noted in several cases in paper I.

Next, one of the weaker towers, called Q, was studied in the same manner and the results are presented in Table VI. The significant feature of Table VI is that a considerably lower buoyancy had to be chosen for this bubble to give the same value of $\overline{G}$ as the others. The buoyancy for this bubble was taken from the moist adiabat shown by the dotted line (left-hand adiabat) on Figure 7, with a correction for weight of hydrometeors of 3 gm/m^3 at 9.72 km diminishing to 2 gm/m^3 at its maximum height of 10.94 km. The resulting values of gB given in Table VI average 0.55 times the values used for X and Y in the height range 10.42-10.94 km. This latter bubble (Q) possessed lower ascent rates and perished sooner than the preceding two described. It can now be seen that it must have been a considerably more dilute bubble, its level of origin being perhaps about 5.9 km or 19,300 ft.

Table V

Tower Y, April 1, 1953

Height range studied 10.25-12.60 km

Observation number	(-t) sec	$(-t)^{\frac{1}{2}}$ $sec^{\frac{1}{2}}$	w mps	$\dot{w}$ cm/sec^2	gB cm/sec^2	$\dot{w}/gB$	$(1-\dot{w}/gB)^{\frac{1}{2}}$	G $sec^{-\frac{1}{2}}$
1	318	17.8	11.7	0	15.5	0	1.00	0.23
2*	300	17.4	11.4	-0.6	14.0	- .04	1.02	0.22
3	282	16.8	10.9	-0.9	13.3	- .07	1.04	0.21
4	264	16.3	10.5	-1.5	12.7	- .12	1.06	0.21
5	246	15.7	10.3	-2.2	11.5	- .19	1.09	0.19
6	228	15.1	10.0	-2.8	10.9	- .26	1.12	0.19
7	210	14.5	9.8	-3.1	9.0	- .35	1.16	0.16
8	192	13.8	9.2	-3.1	8.6	- .36	1.17	0.15
9	174	13.2	8.6	-3.7	8.4	- .44	1.20	0.16
10	156	12.5	7.5	-3.7	8.0	- .46	1.21	0.16
11	138	11.8	6.7	-3.7	7.6	- .49	1.22	0.16
12	120	11.0	6.7	-3.7	7.6	- .49	1.22	0.15
13	102	10.1	6.4	-3.7	7.6	- .49	1.22	0.15
14	84	9.2	6.0	-4.3	7.6	- .56	1.25	0.15
15	66	8.1	5.0	-5.3	7.0	- .76	1.33	0.15
16	48	6.9	3.6	-5.8	6.5	- .90	1.38	0.17
17	30	5.5	2.2	-6.0	5.0	-1.20	1.49	0.19
18	12	3.5	1.0	-7.0	4.0	-1.75	1.66	0.23

*Bubble diameter measured as 2.1 km

$\bar{G} = 0.180$
$\Delta = 45\%$

Table VI

Tower Q, April 1, 1953

Height range studied 9.72-10.94 km

Observation number	-t sec	$(-t)^{\frac{1}{2}}$ $sec^{\frac{1}{2}}$	w mps	$\dot{w}$ cm/sec^2	gB cm/sec^2	$\dot{w}/gB$	$(1-\dot{w}/gB)^{\frac{1}{2}}$	G $sec^{-\frac{1}{2}}$
1*	216	14.7	8.9	0	13.0	0	1.00	0.21
2	198	14.0	8.6	-0.9	12.5	-0.07	1.04	0.21
3	180	13.4	8.4	-1.2	12.0	-0.10	1.05	0.20
4	152	12.3	8.1	-1.6	11.1	-0.14	1.07	0.18
5	144	12.0	7.2	-1.9	10.5	-0.18	1.09	0.19
6	126	11.2	6.4	-2.2	9.8	-0.23	1.11	0.19
7	108	10.4	5.9	-2.8	9.2	-0.30	1.14	0.19
8	90	9.5	5.5	-3.1	8.8	-0.35	1.16	0.18
9	72	8.5	5.1	-3.7	8.4	-0.44	1.20	0.17
10	54	7.4	4.1	-4.3	8.0	-0.54	1.24	0.18
11	36	6.0	3.0	-5.5	7.0	-0.79	1.34	0.19
12	18	4.3	1.8	-6.2	6.0	-1.00	1.41	0.20

*Diameter of bubble measured as 1.3 km

$\overline{G} = 0.191$
$\Delta = 21\%$

rather than cloud base. It presumably formed from smaller bubbles and dilute wake material near this level, while the other two formed near cloud base. Its concomitantly smaller required temperature excess (about 1.3°C compared to about 2.6°C for X and Y) over the surroundings at 5.9 km is consistent with this point of view.

It will be seen by inspection of Figures 3 and 4 that Tower Q rose on the extreme left side of Cloud I (upwind and upshear). In fact at the time it formed, this part of the cloud was almost entirely separate from the larger cloud mass to the right. The average width of its cloud mass was only about 4 km, while Tower Y rose from a cloud mass at least 9 km in width. By the time Tower X rose from the right-hand portion of the cloud, this section had grown until it, too, had attained an average width of about 9 km. These data might thus suggest that, under given conditions, a minimum horizontal cloud dimension is required to permit emergent buoyant elements to rise all the way from cloud base without dilution. Since the undiluted elements will, in general, compose the strongest and most penetrating towers, it may well be that for cumulus to attain a sufficient vertical thickness to give rise to precipitation, a comparable horizontal size must first be attained.

To investigate these points further, the other weak towers put up by Cloud I were studied. There were three such towers detectable on the film. One (P) was too feeble and short-lived to be treated quantitatively. One of the two remaining, called C, appeared on Print 12 (see Table II) just as the bubble studied in Tower Y was closing its life cycle. Although it appeared from the same large cloud mass as did Y, its buoyancy was the same

as that of the diluted tower, Q. It had an active lifetime of 185 secs, a maximum updraft speed of 7.2 mps and a height range of 10.4-11.2 km.

The final tower was the very last one appearing on the film sequence, called R. In order to have the same value of G as the other towers, it had to be slightly dilute and to follow a moist adiabat about half-way between the dashed and the dotted curve on Figure 7. It covered a height range from 10.6-11.85 km, exhibited a maximum updraft speed of 7.8 mps, and a life period of 275 secs, just short of those of the strongest towers. At the time of its emergence, the entire cloud mass of Cloud I was apparently beginning to decay, and although the bubble came from the main portion of the cloud, its horizontal dimension was then only a little over 7 km. Thus it is seen that although the strength of the emerging towers and the dimension of the producing cloud mass in general appear to have some relation, another factor or factors must also be operative, since the largest cloud mass produced weak as well as strong towers. A suggestion concerning one of these factors is made in later paragraphs.

The major features of the towers studied are summarized in Table VII, which also compares observed bubble diameters with the values of their radii of curvature calculated from the Malkus-Scorer model. In the table, the measured diameter of each bubble is compared to the calculated radius of curvature, using both equation (2) and equation (4), for the same frame as the measurement. The earlier work demonstrated that D, so measured, and R came out very nearly equal. The excellent agreement in the present cases gives further support to the applicability of the bubble model. The column marked R_{max} gives the approximate dimension of each bubble as it first emerged from the cloud top, calculated by extrapolation from equation (2).

Table VII

Summary of Towers Studied and Radius Calculations

Tower	Print first appeared	D (meas)	w_{max}	$(-t)^*$	$R = -EgBt^*$	w_o (est. at $-t^*$)	$R=\left(\frac{3}{2} w_o\right)^2 / gB$	R_{max}	Cloud width	Protected range	Unprotected range	Total range	Total lifetime
name-condition	number	km	mps	sec when D meas	km	mps	km	km	km	km	km	km	sec
Y-undilute	6	2.1	11.7	300	2.3	11.4	2.1	~2.5	9	9.6	2.35	12	318
C-dilute	12	0.96	7.2	185	0.85	6.5	1.05	~1	9	4.5	0.8	5.3	185
Q-dilute	23	1.3	8.9	216	1.40	8.6	1.28	~1.3	4	3.8	1.2	5.0	216
X-undilute	34	1.33	11.7	234	1.35	8.3	1.35	~2.1	9	9.8	1.8	11.6	288
P-	39	Too weak to study							9				
R-slightly dilute	50	1.3	7.8	275	1.3	7.3	1.3	~1.3	7	6.0	1.25	7.25	275

It will be noted that the strong, undilute towers, X and Y, had maximum radii in excess of 2 km, while the weaker ones just exceeded one kilometer.

Two of the four weaker towers emerged from smaller cloud masses while the other two emerged from the largest ($\sim$ 9 km) ones. In the case of the latter, namely C and P, one noteworthy feature is held in common. In each case, the weak tower followed its predecessor's emergence after an unusually short interval, 7.2 minutes in the case of C and 6 minutes in the case of P. The strongest towers, Y and X, were separated by more than a half hour, while X and R were separated by nearly 20 minutes. If, as suggested by writers on the bubble model, the larger cloudy bubbles are formed by aggregation of smaller ones at low levels within the cloud, this fact becomes somewhat clarified. A certain time interval is apparently necessary for a sufficient number of small bubbles to accumulate in the low cloud levels in order to form a large vigorous one which can rise to emerge undiluted from cloud top.

The last four columns in Table VII may now be examined. By "protected range" is meant the vertical distance between the level of bubble origin and the cloud top. The level of origin for each bubble was estimated roughly, from Figure 7 in conjunction with the film. The "unprotected range" is the height range studied, or the height range achieved during the active, emergent, isolated life of the bubble. In the case of those bubbles which did not follow their predecessors too closely, the protected range and cloud mass width are very comparable. In the case of all bubbles studied, the unprotected height range and radius at emergence, R_{max}, are comparable, as noted for smaller bubbles in I. It appears that the presence of ice crystals has no noticeable effects upon the bubbles during their

active lives, although it may cause slower dissipation of their wakes and remnants.

The last column on the right shows that the very vigorous undilute bubbles had active lives of about 300 secs or five minutes (X could have been followed this long on the film) and successively weaker bubbles had successively shorter lives. Bubble P probably existed independently for 100 secs or less. In each case, as Tables I-III show, the remnants of the towers went on rising at roughly 1 mps for about 10 minutes more, achieving heights greater than 13 km. Then dissipation set in and occupied another 10-15 minutes without much further ascent taking place.

Since the present discussion has in part concerned undiluted cloud elements, some rising all the way from cloud base moist adiabatically, it must be emphasized that any resemblance to the hypotheses and results of the parcel method is strictly superficial. The parcel method concerns cloud elements which in no way interact with the surrounding air and which would continue to accelerate upward wherever the parcel density is less than that of the environment. In the present case, a rough calculation shows that parcels becoming saturated at cloud base would emerge from cloud top at 10 km with upward velocities well in excess of 60 mps and still increasing! Since the bubble, on the other hand, is hypothesized to be travelling at very nearly its limiting velocity at all times (at least after emergence) its interaction with its surroundings is held to be absolutely vital. In fact the buoyancy force is balanced by form drag (produced by flow around the bubble cap) and is not producing a resultant upward acceleration. On the contrary, the bubble's upward velocity is in general decreasing due to erosion. To summarize: the parcel method prescribes no relations between

the velocity and radius of a convective element and an erroneous relation between velocity, buoyancy and time. The present model suggests quantitative relations between these parameters, which are tested here.

Although the wake production process has not been explicitly examined, it is hypothesized to be the mechanism by which mixing with the surroundings and entrainment of outside air into the main cloud body are occurring. This topic must be the subject of much future work, once the simpler features of the present model have been established quantitatively. Meanwhile certain further deductions concerning interaction of bubbles and environment may be drawn from the present data.

c) The Effects of Wind Shear and the Horizontal Drag on a Bubble

In the case of a bubble ascending through a shearing wind field it was shown in I, Appendix II, that actually equation (5) should be replaced by

$$\frac{3}{2} E^{-\frac{1}{2}} \equiv G = \frac{(-t)^{\frac{1}{2}} \, gB \, (1 - \dot{w}/gB)^{\frac{1}{2}}}{w \, (w^2 + u^2)^{\frac{1}{2}}} \qquad (6)$$

where u is the horizontal velocity of the bubble relative to the air. It was further shown that in most shearing fields the difference between the results of (5) and of (6) would be only about 2%, but that when u is of the same size as w, use of (5) gives about a 20% overestimation of G. Tables I and III indicate that in the present case u is indeed comparable to w, since it ranges from 9-15 mps in the region of strong shear. However, it was also shown that a rate of buoyancy decrease of the magnitude experienced by the present bubbles at these heights should lead to about a 15-20% underestimation of G. Since these errors are compensatory and since the present

observations are probably not reliable to better than 15-20% anyhow, no attempt will be made here to introduce such refinements.

Since we have in Tables I and III and in Figure 6 some measurements of the horizontal tower velocity, u, and also the external wind profile, it may be possible also to test a horizontal equation of motion for the cloud towers. In I, Appendix II, is suggested an equation analogous to the vertical equation of motion with wind shear present, namely

$$\dot{u}_b = - \frac{u}{\sqrt{u^2 + w^2}} K (u^2 + w^2) \tag{7}$$

where u_b is the component of the bubble's horizontal motion along the axis determined by the external wind, u_E; u is the relative motion between bubble and surroundings, namely $u = u_b - u_E$; and the dot indicates time differentiation. The constant K was shown to be the same as K in equation (3), namely $9/4R$. Subtracting $\dot{u}_E$ from both sides of (7), we have

$$\dot{u} = - wU' - \frac{u}{\sqrt{u^2 + w^2}} K (u^2 + w^2) \tag{8}$$

since $\dot{u}_E = wU' = wdU/dz$ and $\dot{u} = \dot{u}_b - \dot{u}_E$ and U' or dU/dz is the external wind shear.

If the bubble has been rising through constant shear for several hundred meters and if it still is fairly near the beginning of its life cycle so that K is changing only slowly, $\dot{u}$ is very small, as is $\dot{w}$, and (8) may be solved approximately to give

$$- \frac{u}{w} \cong \frac{4RU'}{9\sqrt{u^2 + w^2}} \tag{9}$$

after substitution of (3a) for K.

The region of strong shear on Figure 6 corresponds to the earlier phases of the cycles of the towers studied. Hence (9) may be tested. Table I shows that Tower X possessed a u of about -15 mps in this region and Table III gives an average for Tower Q of about -12 mps. Assuming that these bubbles had been rising through the shearing layer long enough for $\dot{u}$ to be very small, and taking the observed U' of 3×10^{-2} sec^{-1}, R for Tower X comes out 1.8 km and R for Tower Q comes out 1.4 km, compared to the calculated values of 2.1 and 1.3 km respectively which appeared in Table VII. These independent results are consistent with the predictions of the model and agree within observational error, although it must be conceded that the measurements and the approximations made are such that this high degree of agreement is somewhat surprising.

It is not clear from the observations whether, as the bubble continues its life cycle, the horizontal drag coefficient increases in the same manner as its vertical counterpart, which the model declares that it should, although this is at least roughly suggested by the fact that $u = u_b - u_E$ seems to be decreasing in magnitude before evaporation sets in and makes it impossible to measure further. Changing wind shear coupled with the difficulty of tracing a single point in its horizontal travel precludes an accurate quantitative test of (8) solved for E (after substitution of $K = 9/4R$ and $R = - EgBt$) such as was done for the vertical equation (3).

In a shearing wind field a rising bubble should have a horizontal as well as a vertical component to its trailing turbulent wake. Earlier observations by Malkus (1949) suggest the presence of such a wake region in the

horizontal, since several hundred feet of "dying cloud" was commonly found on the downshear edge of cumuli.

V. CONCLUSION

The clouds studied in this paper are of interest for two main reasons: first, they are the largest clouds in conditions of strongest shear to which the techniques described here have been applied. Previous clouds investigated by this project have been small or middle-sized trade cumulus and fair weather cumulus of middle latitudes, none of whose tops reached the freezing level. Some similarities and some contrasts between these clouds and the smaller ones studied earlier are striking. The outstanding similarity is the applicability of the same erosion constant, E, to the towers. The predominant contrast is the relatively less important role played by mixing with the clear-air environment in the bigger clouds. This is not to say that interaction between cloud elements and their surroundings is any less important, since it was demonstrated here that the strongest bubbles studied emerged from cloud top with velocities less than 1/6 that of a non-interacting parcel. In fact, it has been indicated that a minimum cloud dimension is necessary to shield the innermost core from dilution. In the case of these clouds, a mass roughly 9 km across (in the plane of the wind and the wind shear) could produce at intervals of about 20 minutes, undiluted bubbles 2 km in diameter which emerged from cloud top rising at 11 mps. The relation between radius, buoyancy, velocity, and lifetime of these elements agreed very satisfactorily with the relations established by the work of Malkus and Scorer in paper I.

The greatest importance meteorologically of the clouds studied is,

however, their role in the over-all picture. It must be supposed that clouds of this type and scale, although rarely observed from the ground due to prevailing overcasts under disturbed conditions, are the rule and not the exception when an extended polar trough reaches down to trade-wind latitudes.

It is well established (Riehl, 1950) that the strong and high-penetrating convective activity which occurs in these troughs is the means by which the upper troposphere receives the major fraction of its latent energy supply. A sample calculation will illustrate the magnitudes involved. Assume that at the 25,000 ft. level, a single saturated cloud tower is active at a given moment in an area 30 km on a side (roughly correct for April 1, 1953). If the updraft speed is 10 mps and the draft is 2 km on a side, continuity will be met by subsidence at 4 cm/sec over the remaining area. Since even the more dilute towers at this elevation have about 3.0 gm/kg water vapor content and the ambient air from the sounding less than 0.5 gm/kg, the net upward transport of water vapor is probably not less than 6×10^7 gm/sec or 3.6×10^{10} cal/sec in latent heat. Distributed over the area involved, this is 400 cal/cm^2 per day. This figure should be compared to a several months' average evaporation rate of 250 cal/cm^2 per day calculated for a similar latitude in the Pacific trade-wind region by Riehl, Yeh, Malkus, and La Seur (1951). Clouds such as these thus play a major role in maintenance of the energy budget of the trades and on that basis alone merit further study.

Acknowledgments

The writers would like to thank Mr. Glenn Stallard and the personnel of the U. S. Weather Bureau at San Juan, Puerto Rico, for their extensive and patient cooperation, and for furnishing much of the basic data used in this study.

They would also like to express deepest gratitude to Professor D. C. MacDowell of the Department of Meteorology of the University of Puerto Rico, without whose continued help and participation their trade-wind investigation could not have been performed.

The enthusiasm of Dr. Herbert Riehl provided the incentive for working up this particular section of the data, and the criticism and valuable ideas provided by Dr. R. S. Scorer were essential in the analysis.

Appendix

Concerning the Applicability of the San Juan Radiosonde and Radio-Wind Data to the Location of the Clouds Studied

Since the clouds are 160 miles away from San Juan, and the midpoint of the observations upon them occurred two hours subsequent to the 1500 GCT sounding, the important question arises whether the wind and temperature structure at the time and place of the clouds might not differ significantly from the San Juan sounding which was used in the calculations.

Since it can be established by investigation of the synoptic situation on this and previous days, that local changes occurring in these two hours are probably insignificant, the question concerns the magnitude of advective changes.

By using the mean wind velocity throughout the levels of interest (9.4-14 km) and projecting backward, the air in the cloud locality at the middle of the run was 100 miles due north of San Juan at the time of the radiosonde. If, for example, the weak stable layer occurring between about 10-11 km (which coincides with the layer of high wind shear) had a slope northward of 1/150, or that common for a middle-latitude frontal system, it would be at a 3500 ft. or approximately 10% different elevation 100 miles to the north, or in other words, the sounding at the clouds would be shifted in height by 10% at the time and place of the observations upon them. In the trade-wind region, a north-south slope this great is almost surely out of the question.

The results of all the calculations taken together further support the contention in this Appendix. A 10% error in sounding heights relative

to cloud heights would give buoyancy errors of about 20% in the region from about 9.7-11.0 km where the buoyancy is decreasing rapidly with height, and no error from there up to near the level where the bubbles ended their cycles. The constancy of G from 9.7 km on up precludes the possibility of such an error, either in sounding, or in cloud heights, unless by chance they should both be in error in a compensating manner. The additional fact that the wind sounding began to shear at just the height that the clouds began to show shear on the film further mitigates against any but a fortuitously compensatory error.

References

Davies, R. M. and G. I. Taylor, 1950: The mechanics of large bubbles rising through extended liquids and through liquids in tubes. Proc. Roy. Soc., London, A, 200: 375-390.

Malkus, J. S., 1949: Effects of wind shear on some aspects of convection. Trans. Am. Geophys. Un., 30: 19-25.

Malkus, J. S., 1952: The slopes of cumulus clouds in relation to external wind shear. Q. J. Roy. Met. Soc., 78: 530-542.

Malkus, J. S., 1954: Some results of a trade cumulus cloud investigation. Woods Hole Oceanogr. Inst. Ref. No. 53-30. J. Meteor. In press.

Malkus, J. S. and R. S. Scorer, 1954: The erosion of cumulus towers. Woods Hole Oceanogr. Inst. Ref. No. 54-5. Unpublished manuscript.

Malkus, W., 1954: Discrete transitions in turbulent convection. Contr. No. 670, Woods Hole Oceanogr. Inst. Proc. Roy. Soc., London, A. In press.

Riehl, H., 1950: On the role of the tropics in the general circulation. Tellus, 2: 1-17.

Riehl, H., T. C. Yeh, J. S. Malkus and N. E. La Seur, 1951: The north-east trade of the Pacific Ocean. Q. J. Roy. Met. Soc., 77: 598-626.

Scorer, R. S. and F. H. Ludlam, 1953: Bubble theory of penetrative convection. Q. J. Roy. Met. Soc., 79: 94-103.

Stommel, H., 1947: Entrainment of air into a cumulus cloud. J. Meteor., 4: 91-94.

Taylor, G. I., 1950: Formation of a blast wave by a very intense explosion. I. Theoretical discussion. II. The atomic explosion of 1945. Proc. Roy. Soc., London, A, 201: 159-186.

Titles for Illustrations

Fig. 1. Time section for San Juan, Puerto Rico, from 1200 GCT March 31, 1953 to 0600 GCT April 2, 1953. The ordinate is height in feet. Winds are plotted in knots, a short barb indicating 5 knots, a long barb 10 knots, and a solid triangle 50 knots. The solid lines are isotachs of wind speed, drawn every 10 knots, with J indicating maxima. The dashed line indicates the base of the westerlies, and the dotted line shows the top of the moist layer. The heavy solid line marked PT indicates the polar trough which passed San Juan moving eastward on March 31, and the solid line marked EW denotes a weak easterly wave which passed San Juan moving westward early on April 1.

Fig. 2. Still photograph from the PBY showing the clouds studied. The arrows indicate the points upon which triangulation was performed. The aircraft was being flown at 6000 ft. toward 293° True and its location is given in Figure 5.

Fig. 3. Selected prints from the motion picture camera on Anegada from which the calculations were made. The bubble followed on Tower Y is shown by the line; Tower W is indicated by a square; Tower C by the arrow alone; Tower Q by the inverted triangle; the streamer on Cloud II by the erect triangle, and Tower X by the X. The camera was pointed toward 22° T throughout the run. The print number is denoted beneath each frame and consecutive prints were 1.2 minutes apart (every twenty frames of the motion picture film, which was exposed at the rate of one frame every 3.6 seconds).

Fig. 4. Additional selected prints from the motion picture camera on Anegada. On Print 40, Tower P is shown by the arrow alone; Tower X is indicated by an X, and the streamer on Cloud II by an erect triangle. Print 44 was the one used in triangulation (compare to Fig. 2). The arrows alone indicate the points triangulated upon (see results in Fig. 5). The arrow alone on Prints 52 and 58 (the last one in the run) shows Tower R. The dissipation of the entire cloud mass may be noted on the last print.

Fig. 5. Scaled map showing results of the triangulation using Figure 2 and Print 44, Figure 4. The camera on Anegada was located at A, pointing in the direction of the dashed arrow (toward 22°). The PBY was located at B, heading in the direction indicated by the solid arrow. The three points indicated by arrows on Cloud I (Fig. 2 and Fig. 4) lie along the line marked "Cloud I" which lies very closely in the plane 290°-110° and 78 miles perpendicular distance from A. The single point triangulated upon in Cloud I lies 66 miles perpendicularly from the plane 290°-110° through A.

Fig. 6. The wind profile plotted from the San Juan radio-wind observation, 1500 GCT, April 1, 1953. These points, marked by circles, were obtained upon reduction of the original data for this purpose. The curve on the left is windspeed in meters per second, that on the right is direction in degrees from true North. The layer of strong shear has been carefully checked and found on the other soundings in the area, and on previous and subsequent soundings at San Juan. The other points, triangles, bars, squares, and X's are horizontal speeds of the various cloud towers, as denoted on the figure.

Fig. 7. Tephigram showing San Juan radiosonde observation, 1500 GCT, April 1, 1953, reduced from the original data to obtain more closely spaced points than that of the teletype transmission. The sounding is given by the solid line. The dashed line is the moist adiabat intersecting the sounding at cloud base (950 mb) used to obtain the buoyancy for the strongest bubbles, and the dotted line is the moist adiabat used in obtaining the buoyancy of some of the weaker bubbles.

Fig. 8. Height of top of bubble in Tower X in km as a function of time in seconds. The time, -t, is chosen as zero when the bubble levels off and becomes fuzzy in appearance on the film. Several points commonly appear on the same horizontal because readings could only be made to the nearest 0.05 cm on the microfilm viewer. Readings were made both in a forward and backward direction on the film and were found to coincide to this degree of accuracy. Velocities were obtained by reading first differences of the heights, and accelerations by taking second differences (see inset graph). Accelerations were checked by the changes in velocity. The calculations made from these curves are presented in Table IV.

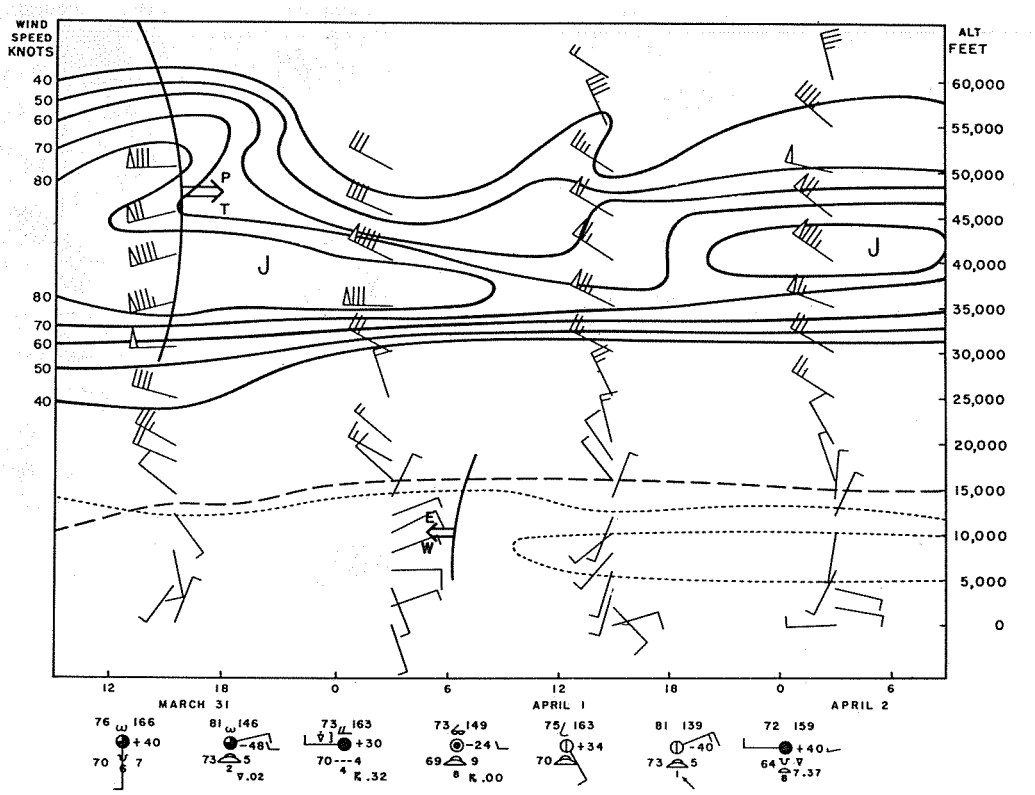

MARCH 31 – APRIL 2 1953 -- TIME CROSS SECTION
SAN JUAN P R

FIG. 1

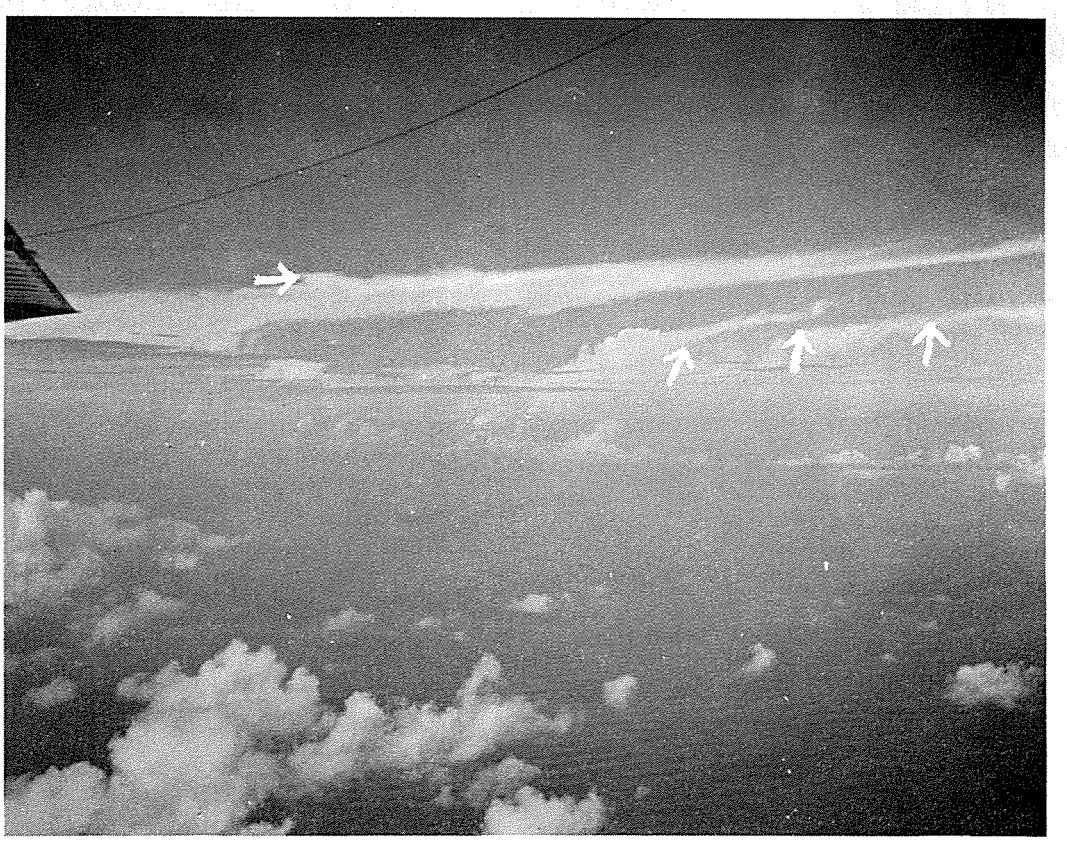

FIG. 2

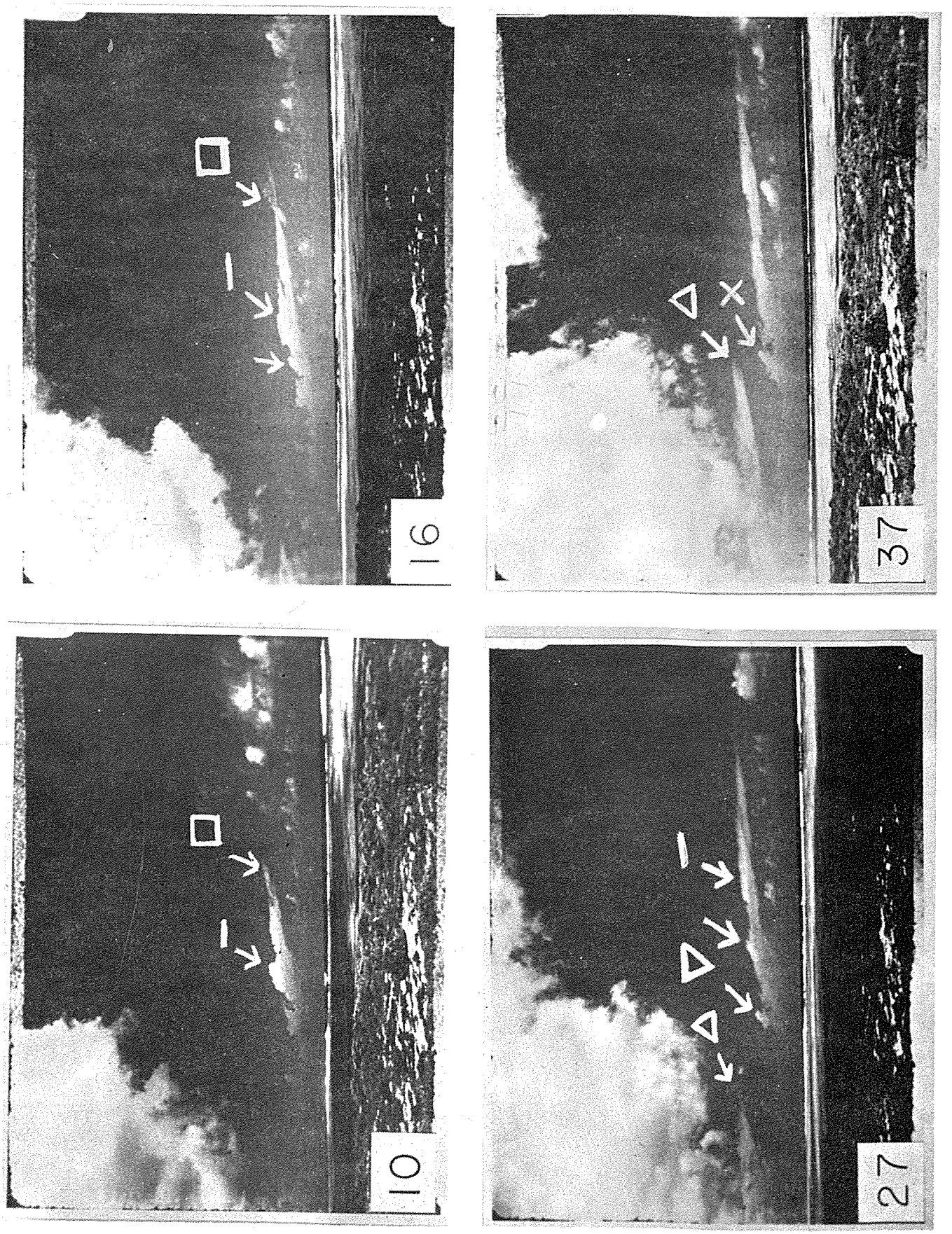

FIG.3

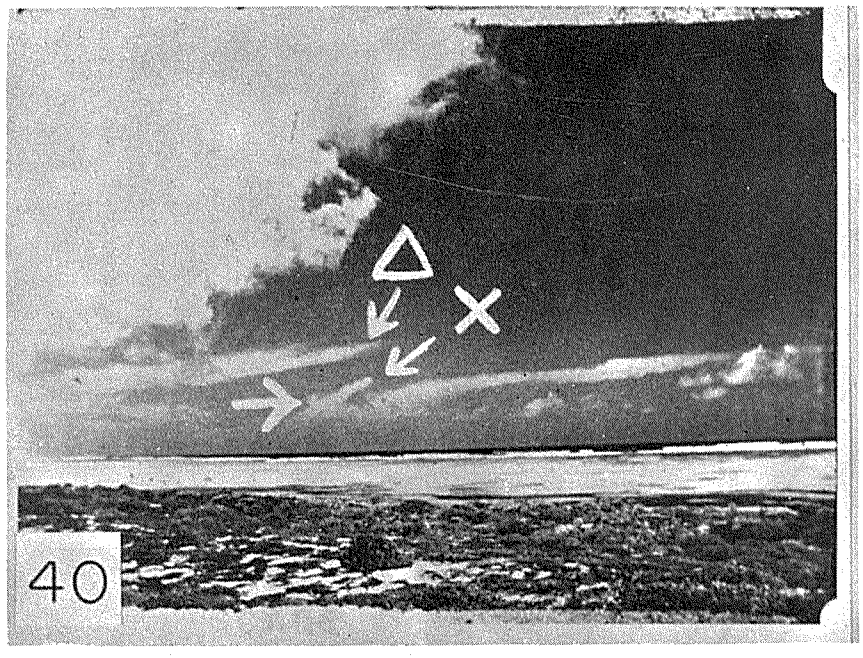

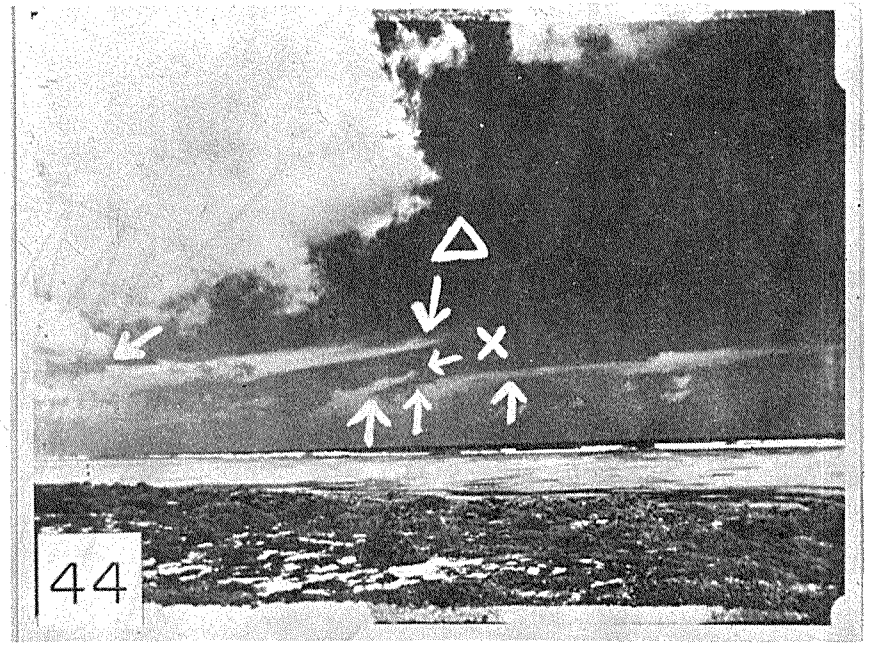

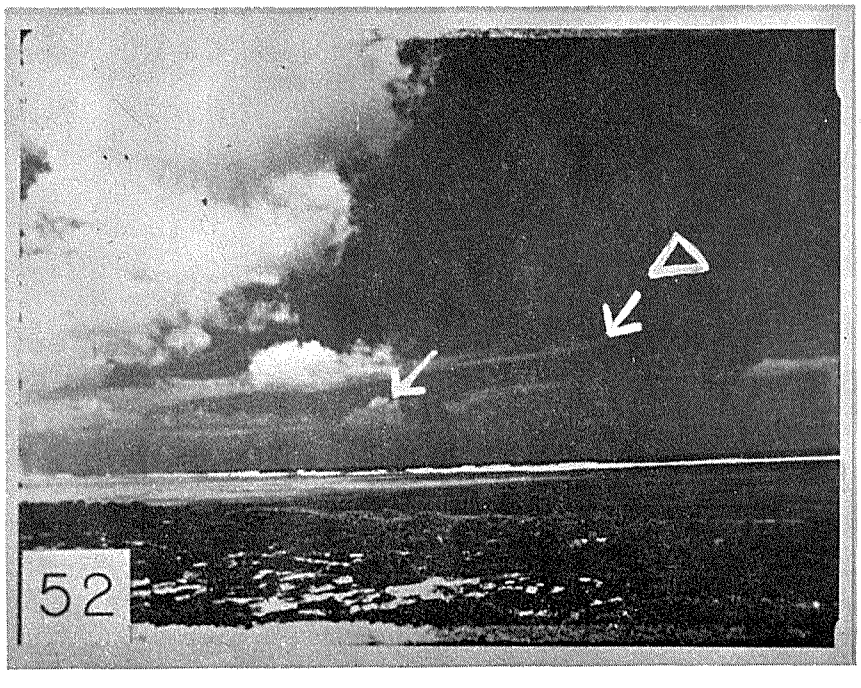

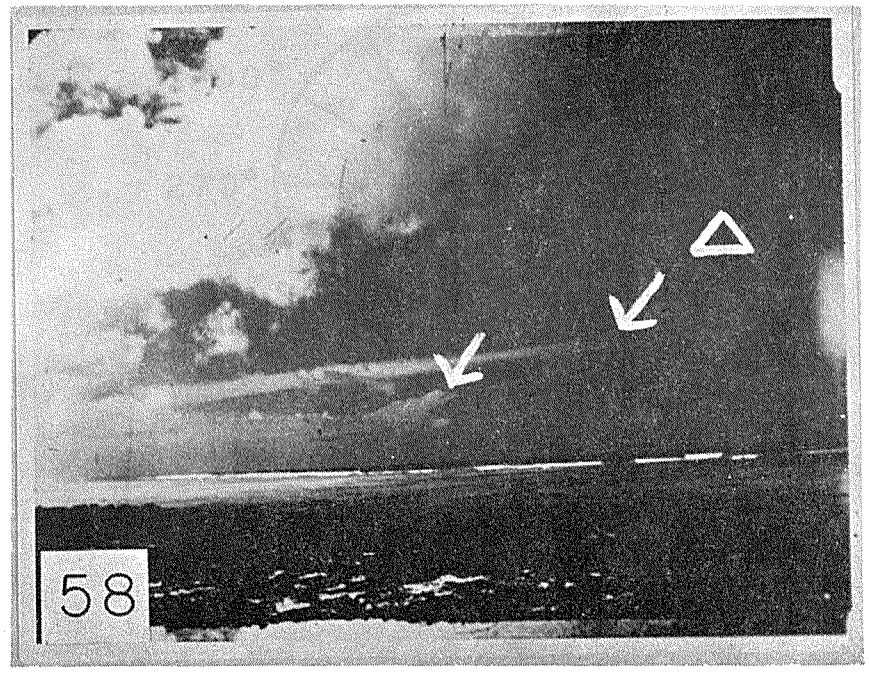

FIG. 4

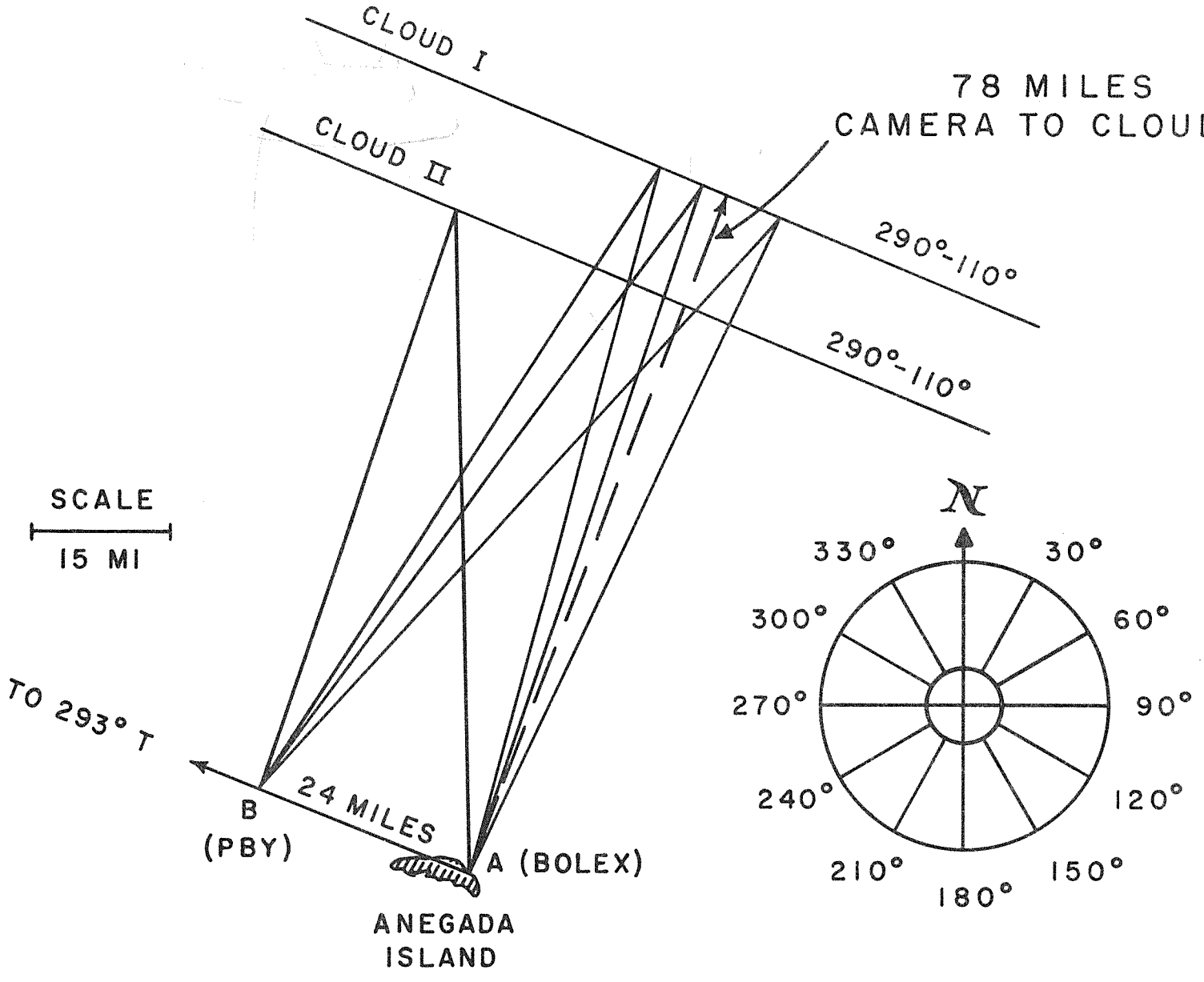

FIG. 5

APRIL 1 1953 – RESULTS OF TRIANGULATION

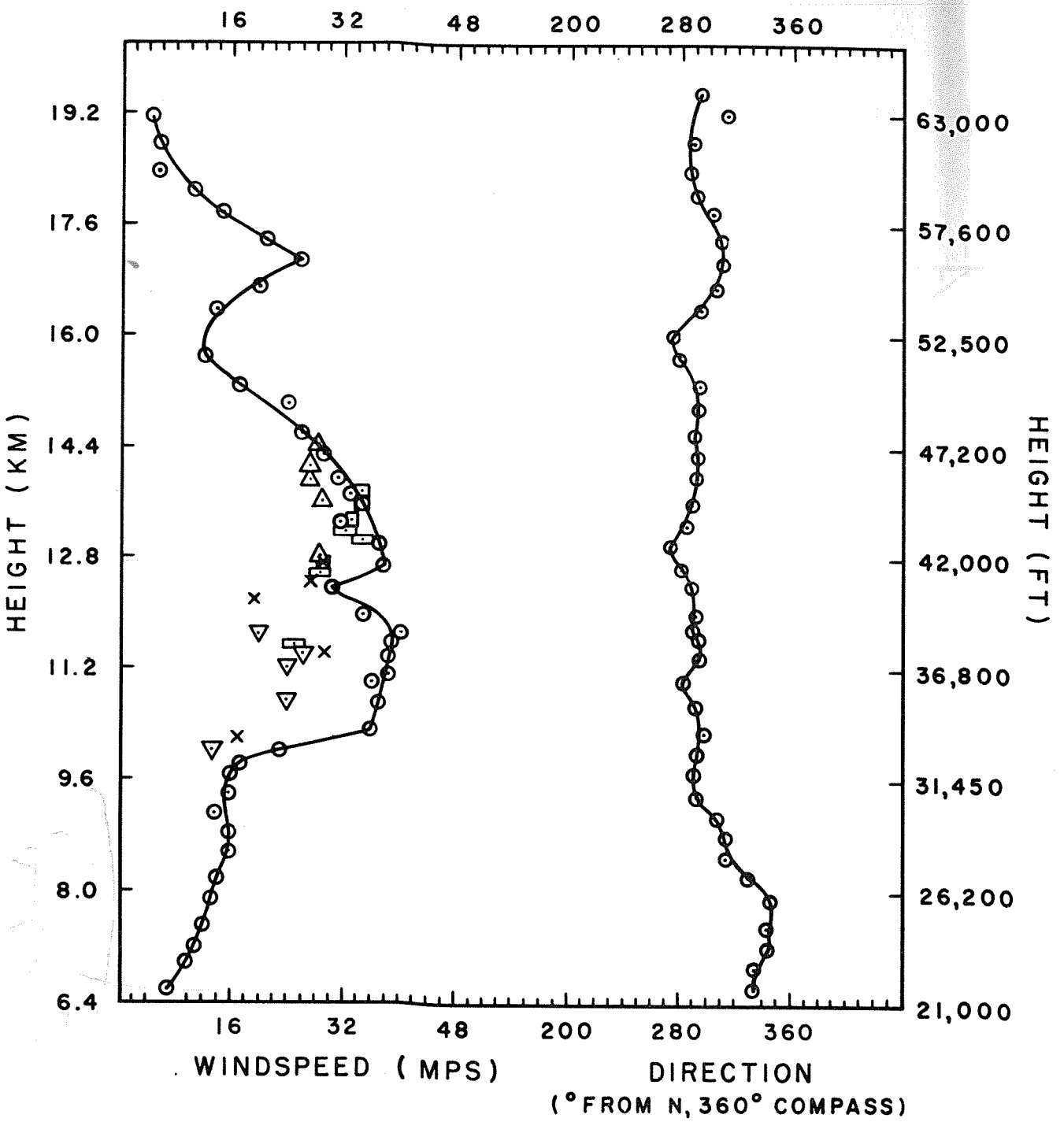

APRIL 1 1953 – RADIOWIND OBSERVATION – 1500 GCT

SAN JUAN P R

FIG. 6

APRIL 1, 1953 RADIOSONDE OBSERVATION

1500 G C T

SAN JUAN PUERTO RICO

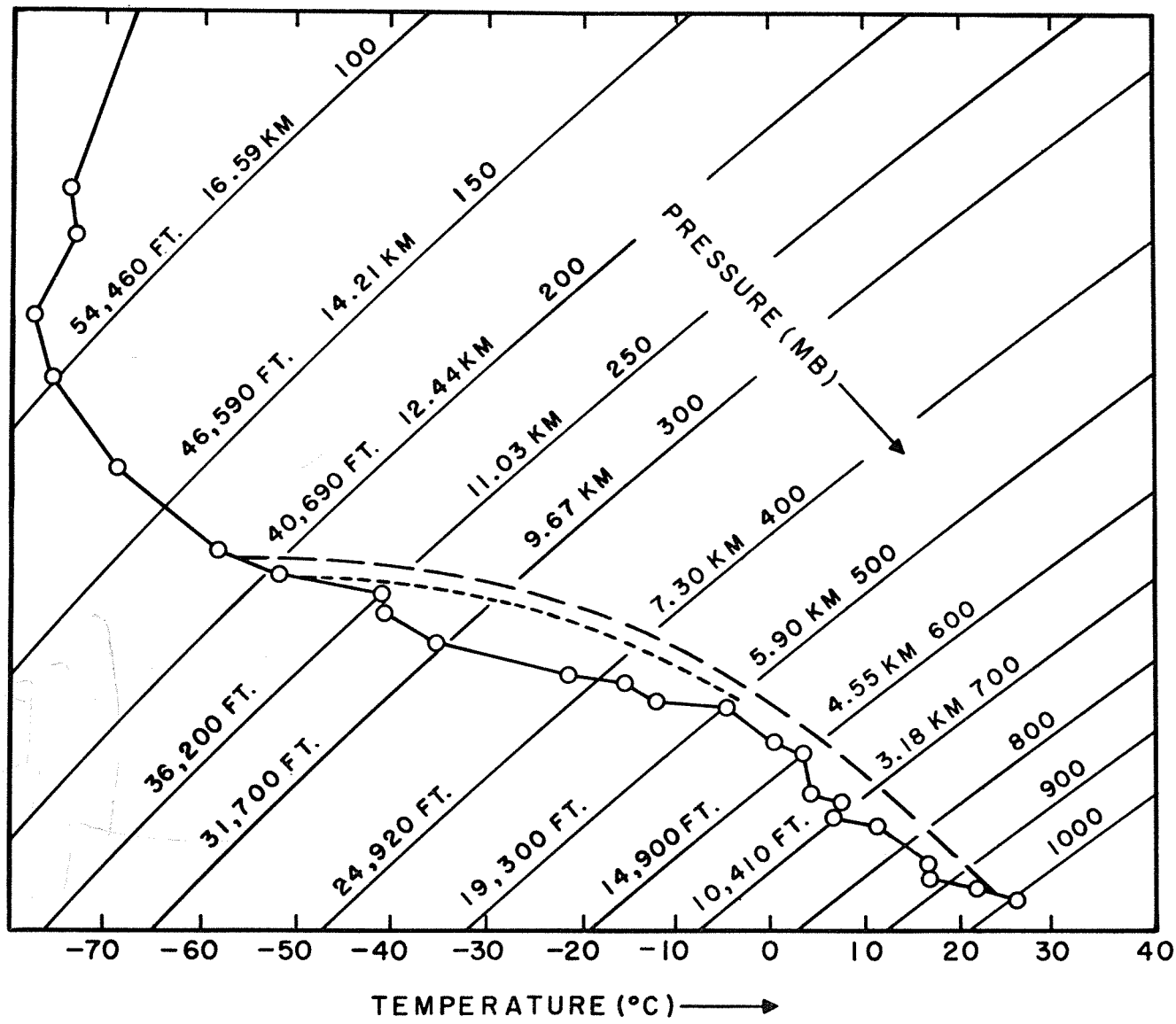

FIG. 7

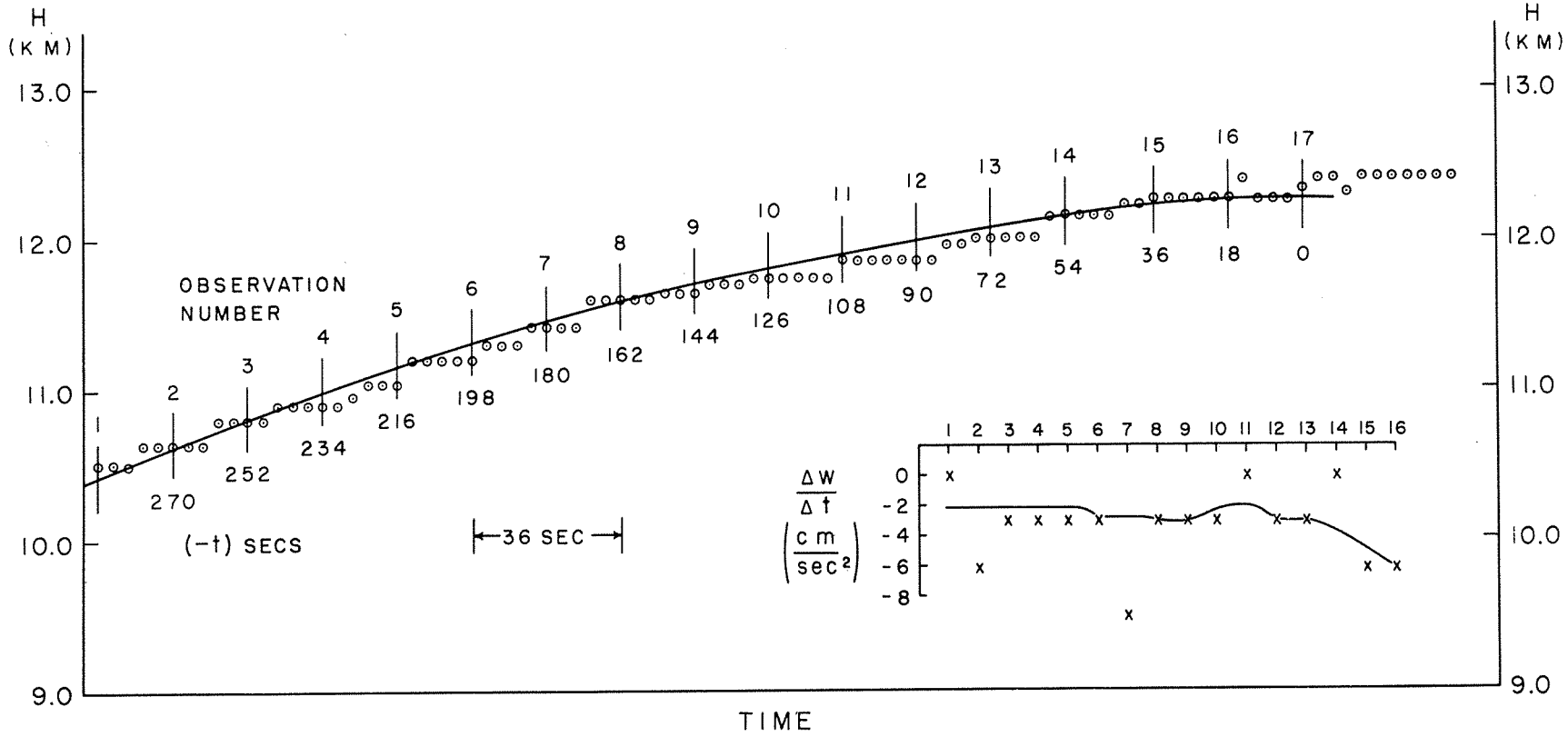

FIG. 8

APRIL 1 1953—TOWER X, CLOUD I

Technical Report Distribution List
ONR Project NR-082-021

24 August 1953

Addressee	Copies
Geophysics Branch, Code 416, Office of Naval Research Washington 25, D. C.	2
Director, Naval Research Laboratory, Attention: Technical Information Officer, Washington 25, D. C.	6
Officer-in-Charge, Office of Naval Research London Branch Office, Navy No. 100, Fleet Post Office, New York, New York	2
Office of Naval Research Branch Office, 346 Broadway, New York 13, New York	1
Office of Naval Research Branch Office, 150 Causeway Street, Boston, Massachusetts	1
Office of Naval Research Branch Office, Tenth Floor, The John Crerar Library Building, 86 East Randolph Street, Chicago, Illinois	1
Office of Naval Research Branch Office, 1030 East Green Street, Pasadena 1, California	1
Office of Naval Research Branch Office, 1000 Geary Street, San Francisco, California	1
Office of Technical Services, Department of Commerce, Washington 25, D. C.	1
Armed Services Technical Information Center, Documents Service Center, Knott Building, Dayton 2, Ohio	5
Assistant Secretary of Defense for Research and Development, Attn: Committee on Geophysics and Geography, Pentagon Building, Washington 25, D. C.	1
Department of Aerology, U. S. Naval Post Graduate School, Monterey, California	1
Aerology Branch, Bureau of Aeronautics (Ma-5), Navy Department, Washington 25, D. C.	1
Mechanics Division, Naval Research Laboratory, Anacostia Station, Washington 20, D. C., Attention: J. E. Dinger, Code 3820	1

Addressee	Copies
Radio Division I, Code 3420, Naval Research Laboratory, Anacostia Station, Washington 20, D. C.	1
Meteorology Section, Navy Electronics Laboratory, San Diego 52, California, Attention: L. J. Anderson	1
Library, Naval Ordnance Laboratory, White Oak, Silver Spring 19, Maryland	1
Bureau of Ships, Navy Department, Washington 25, D. C., Attention: Code 851 (Special Devices Center)	1
Bureau of Ships, Navy Department, Washington 25, D. C., Attention: Code 327 (Technical Library)	2
Chief of Naval Operations, Navy Department, Washington 25, D. C., Attention: Op-533D	2
Oceanographic Division, U. S. Navy Hydrographic Office, Suitland, Maryland	1
Library, Naval Ordnance Test Station, Inyokern, China Lake, California	1
Project Arowa, U. S. Naval Air Station, Building R-48, Norfolk, Virginia	2
The Chief, Armed Forces Special Weapons Project, P. O. Box 2610, Washington, D. C.	1
Office of the Chief Signal Officer, Engineering and Technical Service, Washington 25, D. C., Attn: SIGGGM	1
Meteorological Branch, Evans Signal Laboratory, Belmar, New Jersey	1
Headquarters Quartermaster Research and Development Command. Quartermaster Research and Development Center, U. S. Army, Natick, Massachusetts. Attention: Environmental Protection Division	1
Office of the Chief, Chemical Corps, Research and Engineering Division, Research Branch, Army Chemical Center, Maryland	2

Addressee	Copies
Commanding Officer, Air Force Cambridge Research Center, 230 Albany Street, Cambridge, Massachusetts, Attention: ERHS-1	1
Headquarters, Air Weather Service, Andrews Air Force Base, Washington 20, D. C., Attention: Director Scientific Services	2
Commanding General, Air Materiel Command, Wright Field, Dayton, Ohio, Attention: MCREEO	1
Commanding General, Air Force Cambridge Research Center, 230 Albany Street, Cambridge, Massachusetts, Attention: CRHSL	1
Commanding General, Air Research and Development Command, P. O. Box 1395, Baltimore 3, Maryland	1
Department of Meteorology, Massachusetts Institute of Technology, Cambridge, Massachusetts, Attention: H. G. Houghton	1
Department of Meteorology, University of Chicago, Chicago 37, Illinois, Attention: H. R. Byers	1
Institute for Advanced Study, Princeton, New Jersey, Attention: J. von Neumann	1
Scripps Institution of Oceanography, La Jolla, California Attention: R. Revelle	1
General Electric Research Laboratory, Schenectady, New York, Attention: I. Langmuir	1
St. Louis University, 3621 Olive Street, St. Louis 8, Missouri, Attention: J. B. Macelwane, S. J.	1
Department of Meteorology, University of California at Los Angeles, Los Angeles, California, Attention: M. Neiburger	1
Department of Engineering, University of California at Los Angeles, Los Angeles, California, Attention: L. M. K. Boelter	1

Addressee	Copies
Department of Meteorology, Florida State University, Tallahassee, Florida, Attention: W. A. Baum	1
Woods Hole Oceanographic Institution, Woods Hole, Massachusetts, Attention: C. Iselin	1
The Johns Hopkins University, Department of Civil Engineering, Baltimore, Maryland, Attention: R. Long	1
The Johns Hopkins University, Department of Physics, Homewood Campus, Baltimore, Maryland, Attention: G. Plass	1
New Mexico Institute of Mining and Technology, Research and Development Division, Socorro, New Mexico, Attention: E. Workman	1
University of Chicago, Department of Meteorology, Chicago 37, Illinois, Attention: H. Riehl	1
Woods Hole Oceanographic Institution, Woods Hole, Massachusetts, Attention: A. Woodcock	1
General Electric Research Laboratory, Schenectady, New York, Attention: V. Schaefer	1
Geophysical Institute, University of Alaska, College, Alaska, Attention: C. T. Elvey	1
Blue Hill Meteorological Observatory, Harvard University, Milton 86, Massachusetts, Attention: C. Brooks	1
Laboratory of Climatology, Johns Hopkins University, Seabrook, New Jersey	1
Department of Meteorology, New York University, New York 53, New York, Attention: B. Haurwitz	1
Texas A and M, Department of Oceanography, College Station, Texas, Attention: J. Freeman, Jr.	1
Massachusetts Institute of Technology, Department of Meteorology, 77 Massachusetts Avenue, Cambridge 39, Massachusetts, Attention: T. F. Malone	1

Addressee	Copies
Rutgers University, College of Agriculture, Department of Meteorology, New Brunswick, New Jersey	1
National Advisory Committee of Aeronautics, 1500 New Hampshire Avenue, N. W., Washington 25, D. C.	2
U. S. Weather Bureau, 24th and M Streets, N. W., Washington 25, D. C., Attention: Scientific Services Division	2
Air Coordinating Committee, Subcommittee on Aviation Meteorology, Room 2D889-A, The Pentagon, Washington, D. C.	1
American Meteorological Society, 3 Joy Street, Boston 8, Massachusetts, Attention: The Executive Secretary	1
Research Professor of Aerological Engineering, College of Engineering, Department of Electrical Engineering, University of Florida, Gainesville, Florida	1
The Hydrographer, U. S. Navy Hydrographic Office, Washington 25, D. C.	8

ADDITIONAL DISTRIBUTION LIST

Addressee	Copies
Brookhaven National Laboratory, Upton, L. I., New York, Attention: Meteorology Group	1
Chemical Corps, Biological Laboratories, Technical Library, Camp Detrick, Frederick, Maryland	2
Dr. August Raspet, Engineering and Industrial Research Station, Mississippi State College, State College, Mississippi	2
Dr. E. W. Hewson, Diffusion Project, Round Hill, South Dartmouth, Massachusetts	1
Dr. Hunter Rouse, Director, Iowa Institute of Hydraulic Research, State University of Iowa, Iowa City, Iowa	1

Addressee	Copies
Head, Department of Physics, University of New Mexico, Albuquerque, New Mexico	1
Mr. Wendell A. Mordy, Hawaiian Pineapple Research Institute, Honolulu, Hawaii	1
Dr. E. G. Bowen, Chief, Division of Radiophysics, Commonwealth Scientific Industrial Research Organization, University Grounds, Chippendale, N. S. W., Australia	1
Professor Max A. Woodbury, Department of Statistics, Wharton School, University of Pennsylvania, Philadelphia 4, Pennsylvania	1
Pennsylvania State College, School of Mineral Industries, State College, Pennsylvania, Attention: H. Panosfky	1
University of Wisconsin, Department of Meteorology, Madison, Wisconsin, Attention: V. Suomi	1